Available online at www.sciencedirect.com
SCIENCE DIRECT
Earth and Planetary Science Letters 241 (2006) 104–118
EPSL
www.elsevier.com/locate/epsl

Silicate and carbonate melt inclusions associated with diamonds in deeply subducted carbonate rocks

Andrey V. Korsakov [a,*], Jörg Hermann [b]

[a] Institute of Mineralogy and Petrography of Siberian Branch Russian Academy of Sciences, Koptyug Pr. 3, Novosibirsk 630090, Russia
[b] Research School of Earth Sciences, Australian National University, Canberra, ACT 0200, Australia

Received 8 February 2005; received in revised form 26 September 2005; accepted 27 October 2005
Available online 2 December 2005
Editor: E. Bard

Abstract

Deeply subducted carbonate rocks from the Kokchetav massif (Northern Kazakhstan) recrystallised within the diamond stability field (P=4.5–6.0 GPa; $T \approx 1000$ °C) and preserve evidence for ultra high-pressure carbonate and silicate melts. The carbonate rocks consist of garnet and K-bearing clinopyroxene embedded in a dolomite or magnesian calcite matrix. Polycrystalline magnesian calcite and polyphase carbonate–silicate inclusions occurring in garnet and clinopyroxene show textural features of former melt inclusions. The trace element composition of such carbonate inclusions is enriched in Ba and light rare earth elements and depleted in heavy rare earth elements with respect to the matrix carbonates providing further evidence that the inclusions represent trapped carbonate melt. Polyphase inclusions in garnet and clinopyroxene within a magnesian calcite marble, consisting mainly of a tight intergrowth of biotite+K-feldspar and biotite+zoisite+titanite, are interpreted to represent two different types of K-rich silicate melts. Both melt types show high contents of large ion lithophile elements but contrasting contents of rare earth elements. The Ca-rich inclusions display high REE contents similar to the carbonate inclusions and show a general trace element characteristic compatible with a hydrous granitic origin. Low SiO_2 content in the silicate melts indicates that they represent residual melts after extensive interaction with carbonates. These observations suggest that hydrous granitic melts derived from the adjacent metapelites reacted with dolomite at ultra high-pressure conditions to form garnet, clinopyroxene – a hydrous carbonate melt – and residual silicate melts. Silicate and carbonate melt inclusions contain diamond, providing evidence that such an interaction promotes diamond growth. The finding of carbonate melts in deeply subducted crust might have important consequences for recycling of trace elements and especially C from the slab to the mantle wedge.

Keywords: diamond; carbonate and silicate melts; UHP metamorphism

1. Introduction

Despite the fact that carbonate, carbonate–silicate or carbonate–silicate–sulphide melts have been clearly identified in mantle xenoliths [1–3], the possibility of the formation of such melts in deeply subducted crustal rocks has been discussed insufficiently. Carbonates are present in subducted sediments as well as in subducted continental crust and hence there is plenty of source material to form carbonate–silicate melts. A possible presence of such melts is important for the understanding of metamorphic diamond formation in a subduction zone environment. Recent experiments showed that diamond can form directly from carbonate melts [4,5].

* Corresponding author. Tel.: +7 383 333 25 17; fax: +7 383 333 27 92.
E-mail address: korsakov@uiggm.nsc.ru (A.V. Korsakov).

0012-821X/$ - see front matter © 2005 Elsevier B.V. All rights reserved.
doi:10.1016/j.epsl.2005.10.037

Additionally, carbonate melts are likely to transport different types of trace elements than aqueous fluids or hydrous silicate melts [6–8] and therefore they may produce a different type of sub-arc mantle metasomatism in subduction zones.

Carbonate melts are extremely reactive [2,6,7] and they may be consumed by interactions with country rocks (e.g. metapelites, metabasities). Direct morphological evidence of carbonate or carbonate–silicate melts such as droplets (globule) of carbonate within matrix of contrasting composition [2] is assumed to be only accessible in mantle xenoliths which are essentially quenched during eruption. Exhumation of deeply subducted crust is much slower and is related to extensive recrystallisation of the rocks, hampering the preservation of direct evidence of carbonate melts in subducted rocks. The deepest subducted rocks that are exposed on the Earth's surface reached diamond facies conditions (P~5.0−7.0 GPa, T~1000 °C) [9–12] and provide an excellent natural laboratory to address the question, whether or not carbonatite melts can form in subducted crust. Detailed studies of metamorphic diamonds in metacarbonates from the Kokchetav massif (Northern Kazakhstan) revealed the presence of a fluid phase during diamond formation [13,14]. Polyphase inclusions of hydrous phases together with diamonds in garnet from quartzofeldspathic rocks in the Erzgebirge (Germany) provide evidence for the presence of a hydrous silicate liquid at diamond facies conditions [12,15,16]. While these studies demonstrate the presence of a fluid phase in deeply subducted crust, the nature of these fluids is far from being resolved and no evidence for carbonate melts has been reported so far.

In this paper we present morphological evidence that carbonate melts were included in garnet and clinopyroxene at diamond facies conditions in deeply subducted carbonate rocks from the Kokchetav massif (Northern Kazakhstan). We show with Laser Ablation ICP-MS analyses that the polyphase carbonate inclusions have a different trace element signature than the matrix carbonates. We propose that silicate–carbonate melts are important reactants to produce metamorphic diamonds and we briefly discuss the significance of such carbonate melts for subduction zone processes.

2. Geological setting

The Kokchetav massif (Northern Kazakhstan) represents a slice of continental crust that was subducted to at least 120 km depth, within the diamond stability field [9,17,18]. Recently Massonne [12] estimated a higher peak temperature of 1050−1200 °C. Such high temperatures are in conflict with the observed nitrogen aggregation in diamond [19,20]. For this reason we prefer the more conservative estimates of ~1000 °C. A minimum pressure of 4.3 GPa at 1000 °C is given by the presence of diamond and the maximum pressure of about 6.0 GPa is defined by the stability of dolomite [21,22]. A summary of the geology, tectonic setting and geochronological data for this region has been provided by [18,20,23–28]. The diamondiferous rocks are present in the UHP unit I of the Zerenda Series. This unit consists mainly of garnet–biotite gneisses and schists with alternating marbles, calc-silicate rocks and eclogites [18]. We investigate diamond-bearing carbonates, collected at the classical Kumdy-Kol and Barchi-Kol localities. Additional information on other rocks types can be found elsewhere [29–33]. The high metamorphic conditions recorded in the Kokchetav rocks and the association of metacarbonates and metapelites provide a unique opportunity to study the behavior of deeply subducted mixed crustal materials and to address the question, whether or not carbonate melts can be produced in subducted sediments.

3. Analytical methods

Textural relations were examined in polished thin sections by back-scattered electron images on a Camebax Electron Microprobe (Electron Microscopy Unit, Université catholique de Louvain) and a JEOL 6400 SEM (Electron Microscopy Unit, The Australian National University). The phase compositions were determined on a JEOL 6400 using an energy dispersive detector, an acceleration voltage of 15 kV and a beam current of 1 nA, on a Camebax Electron Microprobe using an acceleration voltage of 15 kV and a beam current of 6 nA (Supplementary Table 1). The trace element contents of minerals and inclusions were analysed in situ by Laser Ablation ICP-MS at the Research School of Earth Sciences [34]. A pulsed 193 nm ArF Excimer laser with 100 mJ energy at a repetition rate of 5 Hz was used for ablation. A mixed Ar–He mixture was used as carrier gas, which was injected into an Agilent 7500 quadrupole ICP-MS for analysis. Spot sizes used for analysis were between 142 and 54 μm depending on the size of the minerals and inclusions. During the time-resolved analysis of minerals, the contamination from inclusions, such as zircon and rutile, fractures and zones of different composition was detected by searching for spikes and changes in the time-resolved spectra of all measured elements and integrating only the 'clean' part of the signal. The relative 1 s deviation of multiple mineral analyses is

generally about 5–20% as shown in Supplementary Table 2. A NIST-612 glass was used as standard material and values were taken from Pearce et al. [35]. Si and Ca derived from microprobe analyses were used as internal standards and a BCR-2G was used as secondary standard.

Mineral abbreviations used in this paper are after Kretz [36], with the exception of the following: Dia—diamond, Coe—coesite, Czo—clinozoisite, Phe—phengite and Zrn—zircon.

4. Petrography of metacarbonates

4.1. Sample description

From a large sample set of carbonate rocks, we selected two of the freshest samples showing peculiar silicate and carbonate inclusions in garnet and clinopyroxene. We have chosen one magnesian calcite (G0) and one dolomite (Car1) marble to investigate the effect of carbonate composition on the composition of phases and inclusions.

Sample G0 contains a compositional layering consisting of different amounts of coarse- to medium-grained clinopyroxene (50–70%), garnet (20–40%), in a magnesian calcite matrix (Fig. 1a,b). Occasionally clinopyroxenes form clusters or bands, and there are lenses consisting of K-feldspar and biotite (up to 5 cm), which are parallel to the compositional zonation in the sample. Clusters of graphite-coated diamonds frequently occur along the contact between garnet and clinopyroxene grains. Large grains of clinopyroxenes have long, fine exsolution lamellae of phengite and phlogopite and more coarse-grained K-feldspar lamellae in their cores. The rim zone of clinopyroxene is free of exsolutions. Similar features have been described for diamond-bearing dolomite marble and diamond-free garnet–clinopyroxene rocks [23,33,37]. In some samples, a first stage of retrogression is documented in exsolution-free clinopyroxene neoblasts, which form mosaic equigranular patches. Some of these clinopyroxene neoblasts are associated with retrograde dolomite and calcite. Symplectites containing clinopyroxene and Al-rich spinel or K-feldspar were identified and indicate that these rocks underwent partly recrystallisation under granulite facies conditions [12,20,23,31,38]. Zircon, rutile and titanite occur as accessory phases.

Dolomite marble Car1 consists of garnet and clinopyroxene embedded in a dolomite matrix. Rutile and zircon occur as accessory phases. Clinopyroxene displays exsolution lamellae of K-feldspar. Garnet contains abundant inclusions of dolomite and rare

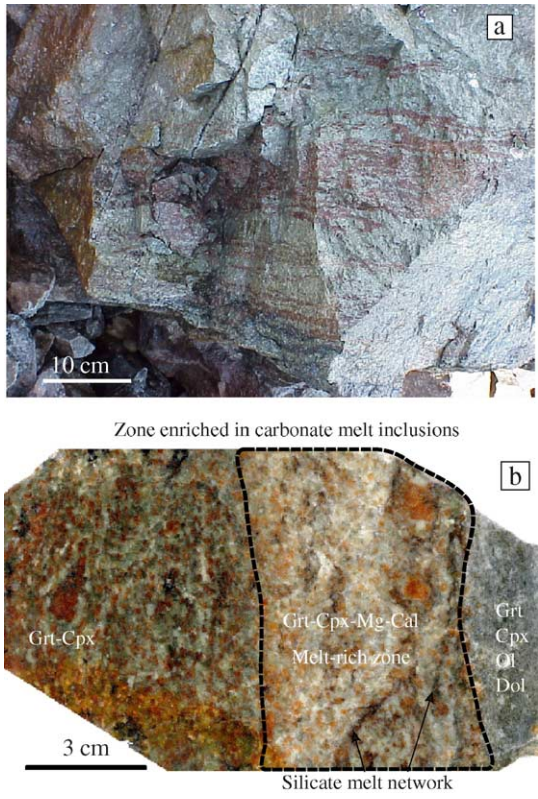

Fig. 1. Outcrop of layered garnet–clinopyroxene rock (a) and a polished slab of the investigated sample G0 (b). Dotted line outlines the melt rich zone, where carbonate and silicate melt inclusions frequently occur.

magnesian calcite. Diamond is mainly present as inclusion in garnet and appears throughout the garnet crystals. Retrograde products include amphibole and biotite which indicate a partly recrystallisation of the dolomitic marble at amphibolite facies conditions [20,23,39].

4.2. Carbonate inclusions

In sample G0, magnesian calcite inclusions are common in garnet and K-rich clinopyroxenes, but are absent in K-free clinopyroxene neoblasts. A small part of magnesian calcite inclusions display rounded shapes and consist of a single crystal, indicating that they represent normal mineral inclusions of the matrix magnesian calcite. However the majority of the inclusions display features, that are very peculiar. About 80% of all carbonate inclusions are polycrystalline and some are associated with other phases such as silicates and diamond. The number of subgrains varies significantly from one inclusion to another. Single inclusions or clusters range from 2 to 300 μm, often displaying regular shapes and occasionally approaching a negative crystal morphology of the host mineral (Fig. 2a). A few

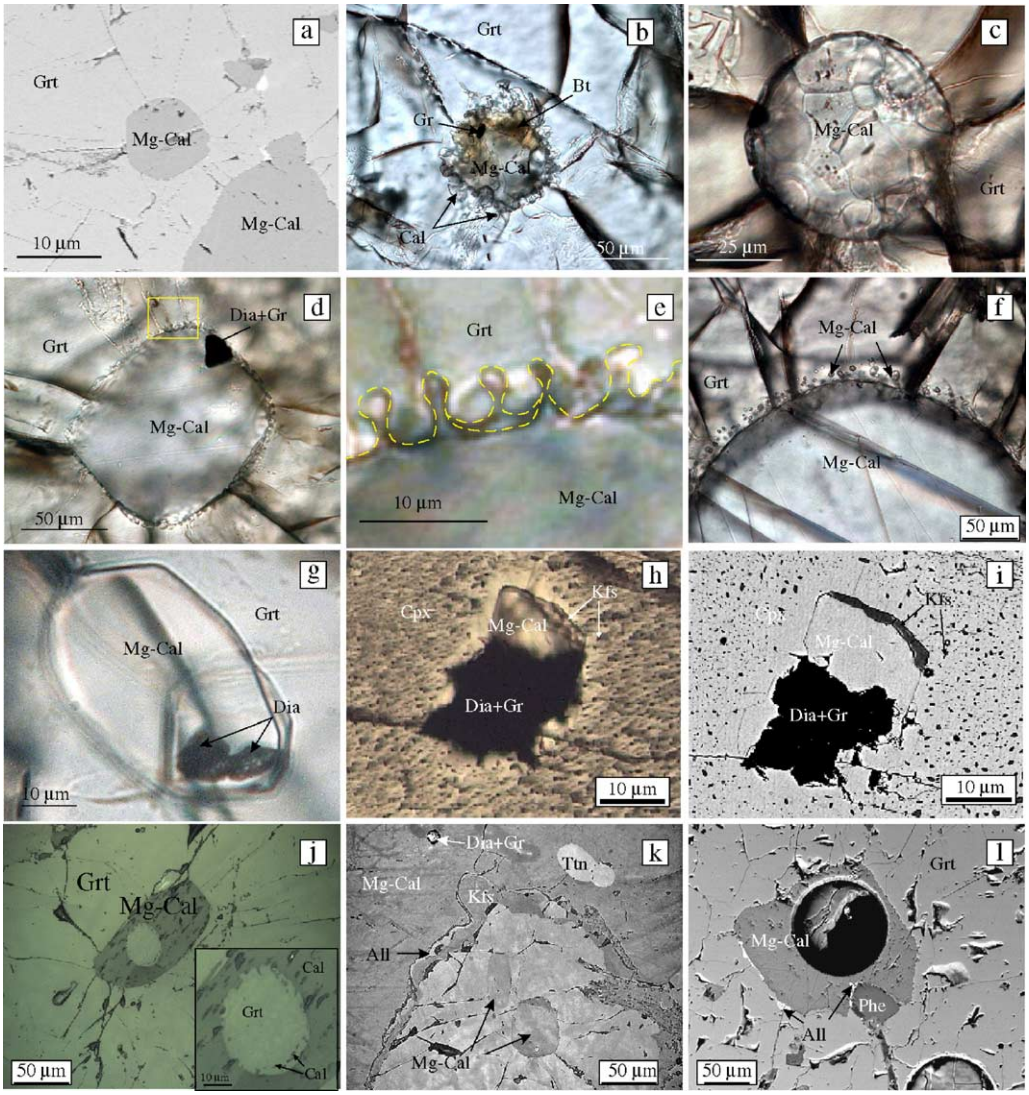

Fig. 2. Polycrystalline and monocrystalline diamond-bearing inclusions of magnesian calcite. (a) Inclusion of magnesian calcite (Mg-Cal) approaching the negative crystal shape of host garnet. (b) Decrepitated carbonate–silicate inclusions in garnet. (c) Polycrystalline inclusions of magnesian calcite probably representing a former carbonate melt inclusions. (d–e) Monocrystalline diamond-bearing inclusions with crown-like wavy boundary with different amplitude of waves, formed by small bulges rooted on the main carbonate inclusion overview and detail, respectively. (f) Main magnesian calcite inclusions in garnet with sharp boundary and surrounded by an aureole of isolated carbonate "droplets". (g) Polycrystalline diamond-bearing magnesian calcite inclusions. (h–i) Intergrowth of subhedral magnesian calcite with graphite-coated diamonds occurring as inclusions in K-feldspar lamellae-rich clinopyroxene (plane polarised light and BSE images, respectively). In the BSE image the lamellae appear as dark spots due to oblique cutting. (j) Small garnet inclusions in magnesian calcite which on its turn is included in a large garnet (reflected light); (k) allanite–K-feldspar overgrowth, separated matrix magnesian calcite and garnet crystal (reflected light); (l) polyphase inclusion (magnesian calcite+Ti-rich phengite+allanite) in garnet from sample Car1.

polyphase inclusions (up to 100 μm) show irregular or rounded shapes and are surrounded by radial cracks, textures characteristic of decrepitation (Fig. 2b,c). Occasionally the magnesian calcite inclusions form a crown-like wavy boundary with the garnet host, formed by small droplets of carbonates rooted from the main inclusion (Fig. 2d,e). Such a texture might evolve into a sharp boundary surrounded by an aureole of separated carbonate droplets (Fig. 2f). Such peculiar textures can best be explained if the carbonate was a liquid phase at the time of entrapment. Diamond inclusions occur in the polyphase carbonate inclusions. They display little (Fig. 2g) or extensive graphite coating (Fig. 2h,i). The K-feldspar exsolution lamellae in the clinopyroxene hosting the diamond-bearing polyphase inclusions are not disturbed by the inclusion (Fig. 2h,i), suggesting

that the inclusion was trapped prior to the formation of the lamellae. Occasionally, small daughter crystals of idiomorphic garnet occur within magnesian calcite that forms an inclusion within a large garnet (Fig. 2j). Abundant calcite inclusions occur along the grain boundary between garnet-daughter crystal and host-calcite and form a crown-like wavy boundary similar to described above (Fig. 2e).

Most of the carbonate inclusions in garnet from the dolomite marble (Car1) consist of dolomite which display a rounded shape. Magnesian calcite inclusions are rare and exhibit straight boundaries to the hosting garnet, indicative of negative garnet crystal shape and are often surrounded by radial cracks. Allanite is often associated with magnesian calcite either in inclusions or at grain boundaries with garnet (Fig. 2k). In one such inclusion, Ti-rich phengite and allanite are associated with the magnesian calcite (Fig. 2l).

4.3. Polyphase silicate inclusions

In sample G0 symplectite-like biotite–K-feldspar intergrowth occurs as inclusions in clinopyroxene, garnets and supersilicic titanite, which is stable at 6–7 GPa and first described by Ogasawara et al. [40]. The ratio of biotite to K-feldspar is nearly constant at 1 : 2. The shape of the inclusions is ellipsoidal in garnet, whereas in clinopyroxene it is rectangular and elongated parallel to the *c*-axis (Fig. 3a–c). Exsolution lamellae of K-feldspar and phengite in clinopyroxene around such inclusions are undisturbed. A biotite–K-feldspar inclusion in garnet contains K-bearing clinopyroxene (Fig. 3b), whereas in clinopyroxene intergrowth with graphite-coated diamond, small garnet and titanite crystals has been observed (Fig. 3d–e). No carbonates were identified within such polyphase inclusions. Another type of polyphase silicate inclusions contains significant amounts of titanite and zoisite together with K-feldspar and biotite. These inclusions display round to oval shapes or rarely they exhibit negative crystal shapes of the host mineral (Fig. 3f). Occasionally, these inclusions display a star-like shape, which is a typical feature of decrepitated fluid/melt inclusions. This second type of polyphase silicate inclusions contains frequently blebs or intergrowth of magnesian calcite. In one occasion, we found such a polyphase

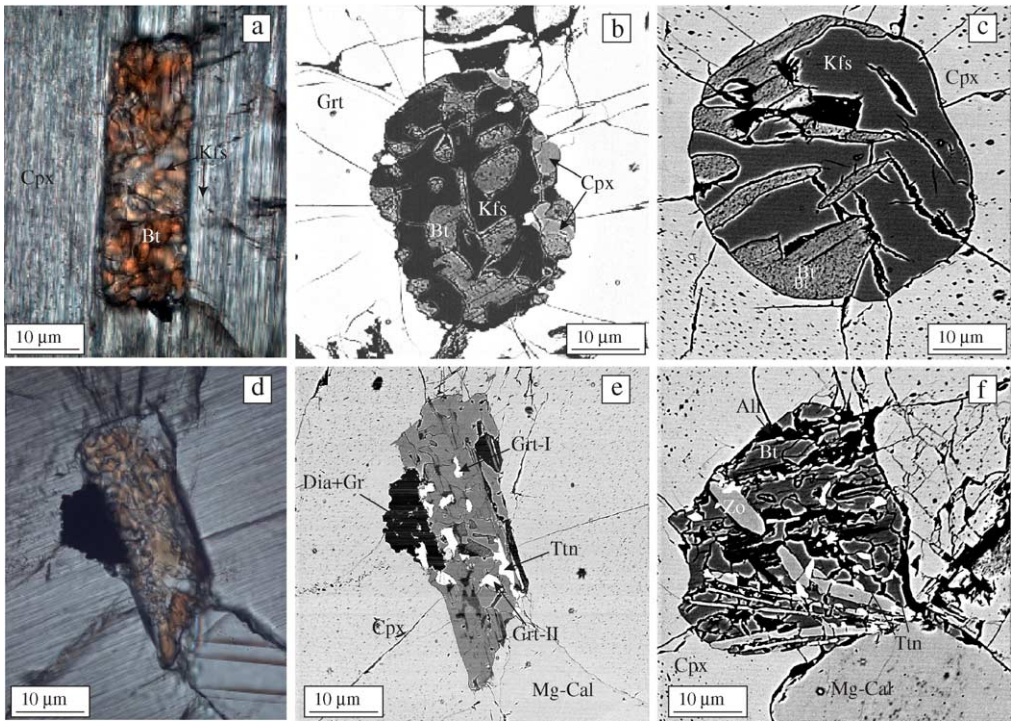

Fig. 3. (a–e) Polyphase inclusions dominated by a biotite–K-feldspar symplectite-like intergrowth with clinopyroxene, garnet and titanite as additional phases. (a) The polyphase inclusion displays a negative crystal shape of host clinopyroxene and is aligned parallel to K-feldspar lamellae. The dark spots in the BSE images (c, d) represent obliquely cut K-feldspar lamellae. (f) Polyphase silicate–carbonate inclusion consisting of zoisite,

silicate inclusion in direct contact with a polyphase Mg-calcite inclusion (Fig. 3f) suggesting a contemporaneous formation of the two inclusion types.

Similar mineral assemblages (kokchetavite (a new polymorph of K-feldspar)+phengite+α/β-cristobalite (or quartz)+siliceous glass ± phlogopite/titanite/calcite/zircon) were recently identified as microinclusions (~1−2 μm) in clinopyroxene and garnet by TEM study [41].

4.4. Diamond and graphite

Diamond and graphite in sample G0 occur in carbonate and polyphase silicate inclusions, in garnet and clinopyroxene and in the intergranular space (Fig. 4). Diamond crystals within carbonate inclusion are generally coated by graphite and mainly appear on the boundary between host mineral and inclusion (Fig. 2d). Some diamond crystals occur in the center of carbonate inclusions (Fig. 2b). The proportion of diamond in the different inclusions is highly variable and can reach up to 90% of the total volume. Graphite rosettes were found in the carbonate matrix of sample G0 (Fig. 4a–b). Occasionally graphite rosettes occur within carbonate inclusion, indicating that their formation process is a primary feature and not related to the retrograde evolution (Fig. 4c–d). In sample G0 large diamonds associated with graphite occur intergranular in the matrix of the carbonate rock (Figs. 2k and 4e). In sample Car1 abundant diamond is present as inclusions throughout garnet (Fig. 4f), indicating that diamond and garnet grew at the same time.

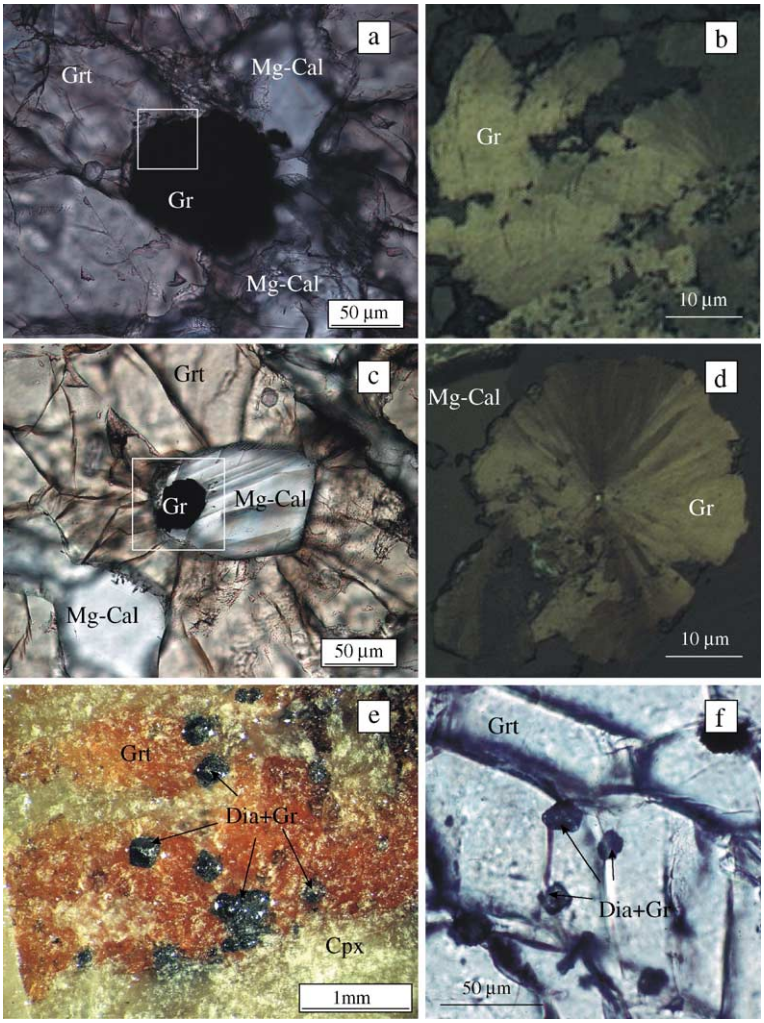

Fig. 4. Morphology of graphite coat formed around interstitial diamond (a–b) and graphite rosettes occurring in magnesian calcite inclusions in garnet (c–d). Inter- and intragranular large graphite-coated diamond crystals from sample G0 (e). Diamond graphite intergrowths inclusion in garnet from carbonate rocks Car1 (f).

5. Mineral compositions

5.1. Garnet

All analysed garnets are characterized by high grossular contents and have a large homogeneous core and narrow rim with different composition. Garnet composition depends on the bulk rock composition. In the dolomite marble, the grossular-component is 48 mol% whereas in the more Ca-rich sample G0, the grossular-component is 56–60 mol% (Supplementary Table 1). The small idiomorphic garnets in the magnesian calcite inclusions have even higher grossular contents of 73 mol%. The pyrope-content increases and grossular-component decreases in the outermost rim of the garnets, whereas the almandine and spessartine content are nearly constant or show a slight enrichment.

The rare earth element (REE) pattern of garnet is very similar in the dolomite and the magnesian calcite marble (Fig. 5). There is a small negative Eu-anomaly. In the main mineral assemblage, garnet is the main host for heavy rare earth element (HREE), and Y and contains significant amounts of P and Ti (Supplementary Table 2).

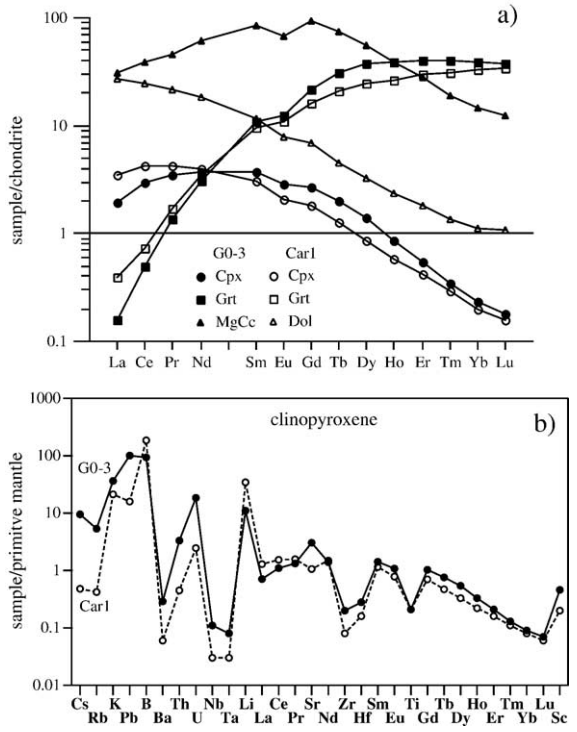

Fig. 5. (a) REE distributions in the minerals from the magnesian calcite marble (G0) and dolomite marble (Car1). Chondrite normalisation after Sun and McDonough [64]. (b) Primitive mantle normalised [65] trace element pattern of clinopyroxene.

5.2. Clinopyroxene

Clinopyroxene composition is close to diopside with very low Al_2O_3 and FeO contents. The jadeite component is generally lower than 5 mol%, reflecting the Na-poor bulk composition of the marbles. The most interesting features in clinopyroxene porphyroblasts are lamella of K-rich minerals such as phengite, biotite and K-feldspar. These lamellae are interpreted to be exsolutions from a K-rich clinopyroxene, stable at UHP conditions [9,25,37]. The K_2O content determined with electron microprobe reaches up to 0.9 wt.% (Supplementary Table 1). Most clinopyroxenes show a weak zonation from core to rim K_2O content decrease from 0.8 to 0 wt.%, whereas FeO and Al_2O_3 increase. The increase of Al_2O_3 is interpreted to be related to restricted recrystallisation during decompression. Clinopyroxene inclusions in garnet display the same features as clinopyroxene porphyroblasts and display K_2O contents up to 1.0 wt.% and in some clinopyroxene inclusions the K_2O content increases from core to rim.

Clinopyroxene displays a HREE depleted pattern indicating chemical equilibrium with garnet (Fig. 5a). A small negative Eu-anomaly is present. Trace element contents of clinopyroxene were determined using a large spot size of 142 μm. This is an elegant way of integrating clinopyroxene and lamellae to obtain the pyroxene composition prior to exsolution. The reconstructed K_2O content is about 1.05 and 0.61 wt.% for the clinopyroxene from the magnesian calcite marble and the dolomite marble, respectively. The primitive mantle normalised pattern display not only extremely high values for K but also for B, Li, Pb and to a lesser extent for Cs, Rb, and surprisingly for U and Th. The clinopyroxene displays negative anomalies of Ti, Nb, Ta, Zr and Hf. The clinopyroxene compositions from the two different marbles are generally quite similar.

5.3. Micas

Biotite and phengite occur as inclusion in peak metamorphic garnet and clinopyroxene in sample G0. The Si content of phengite is about 3.5 (pfu) and TiO_2 contents are about 1.5 wt.%. Biotite contains 4.5 wt.% TiO_2 and has also a relatively high Si content of 3.0 (pfu). Significant trace elements in biotite include 24 ppm Li, 22 ppm B, 713 ppm Rb, 76 ppm Ba and 40 ppm Cs. Phengite contains 20 ppm Li, 176 ppm B, 498 ppm Rb, 35 ppm Ba and 5 ppm Cs. In sample Car1, phengite occurs as inclusion in garnet associated with magnesian calcite (Fig. 2i). This phengite has an extraordinary high TiO_2 content of 5.2 wt.%.

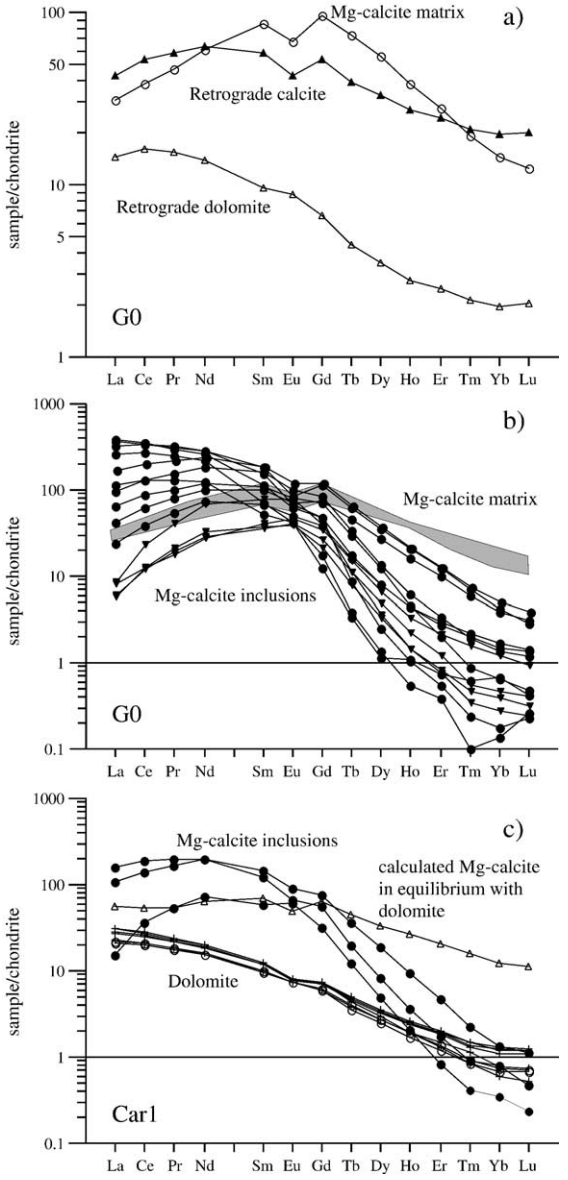

Fig. 6. (a) The REE patterns of peak metamorphic magnesian calcite matrix (open circle) and retrograde calcite (filled triangle) and dolomite (open triangle) in sample G0. (b) REE patterns of matrix (grey field) and polyphase carbonate inclusions with high LREE (filled circle) and three inclusions with abnormal, lower LREE contents (filled triangle) from sample G0. (c) REE patterns of dolomite matrix (open circles), dolomite inclusions (cross) and magnesian calcite inclusions (filled circle) from the sample Car1. Also shown are calculated trace element contents of a hypothetical magnesian calcite (open triangle), that would be in equilibrium with the major phases garnet, clinopyroxene and dolomite.

5.4. Matrix carbonates

Matrix dolomite in sample Car1 is homogeneous and has the composition $Ca_{0.5}Mg_{0.47}Fe_{0.03}CO_3$. The REE pattern shows a pronounced LREE enrichment (Figs. 5 and 6). Dolomite contains about 120 ppm of Sr and 7 ppm of Pb and Ba. MgO contents in magnesian calcite vary slightly and reach a maximum of 2.5 wt.%. The magnesian calcite in G0 contains more REE, Sr and Pb but less Ba than the Car1 dolomite (Supplementary Table 2). Magnesian calcite and dolomite both show a small negative Eu-anomaly. For comparison, we also analysed calcite and dolomite that is associated with retrograde clinopyroxene in sample G0 (Fig. 6a). Retrograde calcite displays a similar LREE concentration as the Mg calcite but lower MREE and higher HREE. The increase in HREE concentration is interpreted to reflect break down of garnet, which is observed in these retrograde zones. Retrograde dolomite displays a similar shape of the REE pattern but has overall lower REE than the calcite. Ba concentrations in both retrograde carbonates are low (<3 ppm).

5.5. Carbonate inclusions

Rounded, single-crystal magnesian calcite inclusions in garnet and clinopyroxene display identical trace element contents as the matrix carbonate. However, the polyphase magnesian calcite inclusions in sample G0 display much higher Ba contents than the matrix carbonates (Fig. 7). Additionally the REE contents of these inclusions are variable and are significantly different from the matrix carbonates (Fig. 6b). Also, the composition of these inclusions display higher LREE and lower HREE contents than retrograde calcite. While retrograde dolomite occurs outside the inclusions, no such dolomite has been found within the inclusions. Moreover, the MREE content of retrograde

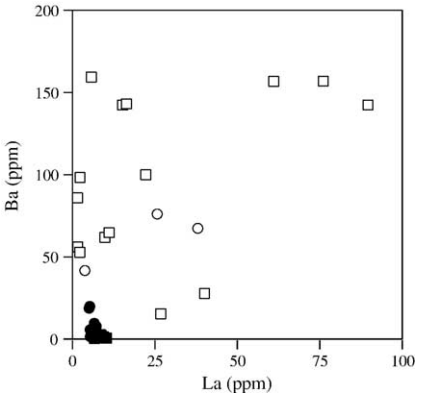

Fig. 7. The Ba and La contents of inclusions (open symbols), that show textures compatible with trapped melt, are much higher than of matrix carbonates (filled symbols). Sample G0: squares; sample Car1: circles.

dolomite in sample G0 is distinctively lower than the polyphase inclusions (Fig. 6a,b). All these observations indicate that the polyphase inclusions do not represent alteration products of normal single-crystal magnesian calcite inclusions. It is not clear whether the variation in the composition is related to incomplete sampling of the different subgrains in the polycrystalline inclusions, or if more than one phase was originally trapped in the inclusions. If the first hypothesis is correct, the appropriate composition of the original phase is the average of all analyses. The primitive mantle normalised trace element pattern of this average is given in Fig. 8a. If the second hypothesis is correct, then the peculiar composition is caused by the phase that is high in Ba and La. The filled squares in Fig. 8a show the average of the three analyses with the highest Ba and La from Fig. 7.

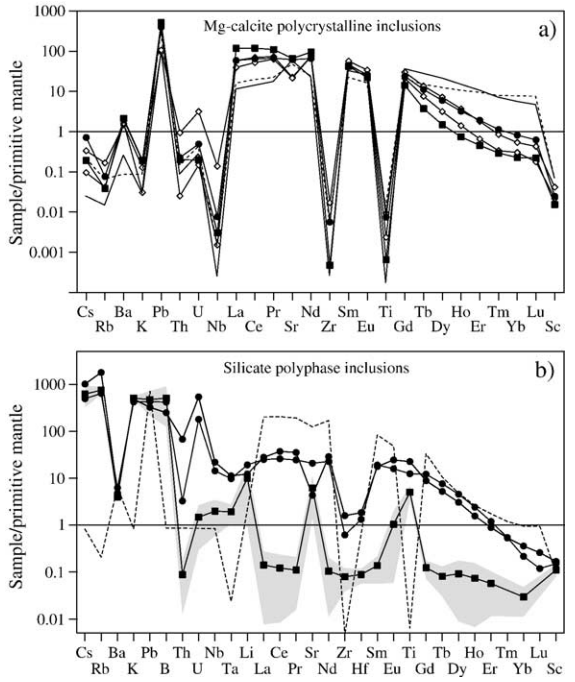

Fig. 8. (a) Primitive mantle [65] normalised trace element patterns for polycrystalline magnesian calcite inclusions. Filled circles represent the average of all inclusions from sample G0 shown in Fig. 6b. The filled squares correspond to the average of the three analyses with highest La and Ba contents. For comparison the compositions of matrix carbonates (solid line) and retrograde carbonate (dashed line) are shown. Open diamonds represent the best obtained analyses of sample Car1. Note the similarity between the trace element patterns of magnesian calcite inclusions in the two samples. (b) Average trace element composition of polyphase inclusions consisting of biotite and K-feldspar intergrowth (filled square). The gray range corresponds to the 1 sigma standard deviation of these analyses. Filled dots represent the best analyses of zoisite–titanite–biotite–K-feldspar polyphase inclusions. The composition of high Ba and La carbonate melts is shown for comparison (dashed line).

The primitive mantle normalised pattern of this average is only slightly different from the composition of the inclusions determined in the other way. The primitive mantle normalised trace element pattern of these polyphase inclusions display strong negative anomalies for HFSE. There is a small negative Sr anomaly, Cs, Rb and K are lower whereas Pb, B and Ba are significantly higher than primitive mantle values. The normalised U content is higher than the Th content. These trace element patterns clearly differ in the HREE, LREE and Ba contents from matrix and retrograde calcite, which also show a positive Sr anomaly (Fig. 8a).

The dolomite inclusions in sample Carl display identical trace element patterns as the matrix dolomite. In contrast, the magnesian calcite inclusions are much more enriched in LREE and MREE with respect to the matrix dolomite and display slightly lower HREE (Fig. 6c). This difference might be caused by a different affinity of dolomite and magnesian calcite for trace elements or because the magnesian calcite represents a quenched carbonate melt as suggested by the textural observations. The Ba content of the magnesian calcite inclusion is very similar to the ones found in sample G0 (Fig. 7). The composition of a fictive magnesian calcite has been calculated in sample Carl using the REE composition of clinopyroxene and the REE partitioning between matrix magnesian calcite and clinopyroxene established in sample G0, where the two minerals are in equilibrium. The result shows that the composition of the inclusions are LREE enriched and HREE depleted with respect to the fictive magnesian calcite that would be in equilibrium with clinopyroxene and garnet. This feature is very similar to what has been observed in the magnesian calcite inclusions in the sample G0. The primitive mantle normalised patterns of the magnesian calcite inclusions display the same key features as the pattern obtained from sample G0 (Fig. 8a).

5.6. Polyphase silicate inclusions

The textural relationships suggest that the polyphase silicate inclusions were trapped as a single phase during garnet and pyroxene growth, which recrystallised to the observed mineral intergrowth during the retrograde metamorphic evolution. The major element composition of the original UHP phase has been determined by combining the major element analyses with the modal abundances of phases. Both types of silicate inclusions have bulk compositions that do not represent any known solid phase (Supplementary Table 1). The biotite–K-feldspar intergrowth contains 54–60 wt.% SiO_2, 13–16 wt.% K_2O and 17 wt.% Al_2O_3 (Supplementary

Table 1). The calculated H_2O contents vary from 0.5 to 1.5 wt.%. The biotite–zoisite–titanite intergrowth contains about 49 wt.% of SiO_2, 11 wt.% K_2O and 17 wt.% Al_2O_3 and significantly higher Ca contents of 4 wt.%.

The trace element contents of the polyphase silicate inclusions have been determined using a large spot size of 86 μm and drilling about 20 μm into the inclusion. The laser ablation analyses thus represents the average of a sample volume, integrating the different minerals present in the intergrowth. The trace element contents of the titanite–biotite–zoisite inclusions display a regular pattern when normalised to primitive mantle values (Fig. 8b). There is an enrichment of large ion lithophile elements (LILE), high concentrations of LREE and a HREE depletion, which is very similar to the pattern in the carbonate inclusions. The normalised Ti content is very similar to REE with similar compatibility. There is a small negative Sr and a significant negative Zr and Hf anomaly and there is a pronounced enrichment of U with respect to Th. The trace element pattern of the K-feldspar–biotite intergrowth displays a very similar LILE pattern as the titanite–biotite–zoisite inclusions. However, the REE contents are at least an order of magnitude lower. There are positive Sr, Eu and Ti anomalies.

6. Discussion

6.1. Ultra high-pressure silicate and carbonate melts

We have observed peculiar inclusions in garnet and clinopyroxene from a magnesian calcite and from a dolomite UHP rock from deeply subducted continental crust in the Kokchetav massif. These inclusions display four prominent features that make them distinct with respect to normal single-crystal mineral inclusions: 1) the shape of the inclusion approaching negative crystal shapes of the host mineral; 2) the fact that they are polyphase inclusions; 3) the fact that they have a trace element composition that is not found in matrix and retrograde carbonates and silicates; and 4) the composition of the peculiar magnesian calcite inclusions is very similarly independent whether they occur in a dolomite or a magnesian calcite marble. These features are best explained by the entrapment of carbonate and silicate melts by garnet and clinopyroxene. Crystallisation of such liquids is likely to produce polycrystalline or even polyphase inclusions, as different crystals form during cooling. This has been convincingly demonstrated in polyphase silicate melt inclusions in garnet from quartzofeldspathic rocks from the Erzgebirge [12,15,16]. Additionally, radial cracks around inclusions, star shapes morphology and aureole of separated carbonate droplets can be best explained as different stages of decrepitation of fluid/melt inclusions [2]. Unfortunately the presence of these cracks indicates that most of the hydrous component likely present prior to decrepitation of the inclusions was lost during the retrograde evolution. Dr. A. Tomilenko (Tomilenko, unpublished data) performed some homogenisation experiments for similar carbonate–silicate inclusions in garnet from the diamond-bearing rocks (Kokchetav massif). He observed decrepitation of such inclusions at 800–850 °C, demonstrating that these inclusions are impossible to rehomogenise, which would be the ultimate test to prove that they were trapped as melts.

There are several lines of evidence indicating that silicate and carbonate melts were present at peak metamorphic conditions. Polyphase silicate and carbonate inclusions are incorporated in supersilicic titanite and K-rich clinopyroxene (~1 wt.% K_2O), which are interpreted to have formed at peak metamorphic conditions [9,23,37,40,42]. Lamellae of K-rich phases (K-feldspar, phengite, phlogopite) in clinopyroxene around such inclusions are undisturbed indicating that the inclusions were trapped prior to the retrograde evolution causing the exsolution. Some diamonds in the carbonate and polyphase silicate inclusions can be considered as daughter crystals. Hence, the melts must have been trapped within the diamond stability field under UHP conditions. It is possible that some additional portions of carbonaceous melt could have been produced by decompression melting from UHP conditions as is generally observed in mantle rocks [22].

Partial melting of diamond-bearing metapelites from the Kokchetav massif has been proposed on the basis of geochemical studies [23,24]. From the detailed study of zircon growth zones it has also been suggested that melt was present during UHP metamorphism [20]. In order to explain the presence of K-rich clinopyroxene in marbles, it has been suggested that a K-rich, probably carbonate-bearing liquid, was present during UHP metamorphism [37] but neither the exact chemical composition of the liquids nor textural evidence has been found so far. The textural, mineralogical and chemical data shown here provide for the first time evidence that there were silicate and carbonate melts present in the deeply subducted marbles from the Kokchetav massif at peak metamorphic conditions of 4.5–6.0 GPa and ~1000 °C.

6.2. Melt generation

Polyphase carbonate and silicate inclusions occur in the UHP domain of garnet and clinopyroxene indicat-

ing the presence of both carbonate and silicate melts during mineral growth. Coexisting carbonate and silicate melts in ultramafic xenoliths have been interpreted to represent immiscible liquids that evolve from one single fluid phase [1,2]. In analogy, contemporaneous carbonate and silicate melts in the UHP marbles suggest that liquid immiscibility might occur in such a chemical system (Fig. 3f). It is not clear, whether immiscible liquids were present at peak or formed during initial decompression. Experimental studies have shown that at very high pressures, such as encountered by the marbles and in the presence of H_2O, liquid immiscibility gaps might close [43,44]. In such a scenario, the carbonate, REE-rich silicate and the REE-poor silicate melt could have formed from one single fluid phase during decompression. The observation that all these different inclusion types are present in UHP phases implies that immiscibility would have occurred still under UHP conditions.

The composition of polyphase silicate and carbonate inclusions is different from the minerals found in the matrix, consistent with a melt origin. However, because of the relatively slow exhumation history of the Kokchetav rocks when compared with xenoliths, it is likely that the trapped melts reacted with the host minerals to a certain extent during crystallisation. Hence, the measured compositions represent a fingerprint rather than the exact melt compositions. Extensive reaction during crystallisation seems unlikely as a systematic difference in REE compositions of polyphase inclusions hosted in garnet and in clinopyroxene is not observed. Moreover, the carbonate melts hosted in the Mg-calcite and the dolomite marble have very similar major and trace element compositions (Fig. 8a). There is no direct experimental proof that carbonate melts can form in garnet–pyroxene bearing marbles at the inferred UHP conditions of ~1000 °C and 4.3–6 GPa. However, there are some experiments in anhydrous carbonate bearing eclogites that display the same phase assemblage (but with different compositions) at these conditions. The study of Dasgupta et al. [45] suggests that carbonate melts might form at 1000 °C, 4.0 GPa. Hammouda [46] suggested that minimum pressures of 6.0 GPa are required to form carbonate melts at 1000 °C. In contrast, in similar experiments, Yaxley and Brey [47] did not find any melt at conditions comparable to the ones encountered by the Kokchetav massif. Hence more high-pressure experiments especially in hydrous silicate–carbonate systems are needed to understand better the formation conditions of carbonate melts. The silicate polyphase inclusions display two distinct major and trace element compositions. Also in this case it is not clear whether these inclusions represent melts that evolved from one single composition through immiscibility or whether they represent two distinct compositions. The compositions of the polyphase silicate inclusions display some similarities to hydrous felsic melts. The main components are Si, Al and K and both inclusion types display high LILE contents and $U_N > Th_N$. However, the SiO_2 content is generally much lower than in felsic melts, which is likely due to the SiO_2 poor carbonate environment. The presence of silicate melt in carbonates is unusual and we suggest that these melts were generated in the neighboring metapelites rather than in the carbonates. As outlined above, there is good evidence that the metapelites, which enclose the carbonate lenses, underwent partial melting at UHP conditions and generated hydrous granitic melts. Such hydrous granitic melts are very reactive with dolomite and are able to produce metasomatic garnet and clinopyroxene in marbles. This is supported by textural observations. Micro-diamond occurs throughout garnet and clinopyroxene crystals. This indicates that these minerals did not grow during prograde metamorphism, as expected in impure marbles, but close to the peak in the diamond stability field by a metasomatic reaction. Moreover, clinopyroxene trace element patterns display very similar features with respect to the silicate melts with high Pb, B and Li and elevated LREE and U contents (Fig. 5b), indicating meta-sedimentary rocks as source for the metasomatic agent. All the main minerals in the Mg-calcite and dolomite marble display a small negative Eu-anomaly (Fig. 5a). Peak metamorphic zircon in the gneisses that likely formed in the presence of melts also display such a negative Eu-anomaly [20]. We suggest that the Eu-anomaly in the marble results from the interaction with melts derived from the gneisses. To summarise the observations, we propose the following reaction:

$$\begin{aligned}&\text{Dolomite} + \text{Hydrousgraniticmelt} \rightarrow \text{Garnet} + \\ &\text{Clinopyroxene} + \text{Ca} - \text{richcarbonatemelt} \pm \\ &\text{diamond} \pm \text{residualsilicatemelt}. \end{aligned} \quad (1)$$

In the dolomite marble, the silicate melt component reacted away leaving a diamond-bearing rock consisting of dolomite, garnet and K-bearing clinopyroxene with rare carbonate melt inclusions. In the calcite marble, the dolomite component has reacted completely leaving a residue with magnesian calcite, garnet, K-bearing clinopyroxene and abundant carbonate melt inclusions as well as a residual silicate melt. The similar REE patterns of garnet and clinopyroxene in the calcite and dolomite marbles indicate that they reacted with a

similar type of silicate melt. The trapped melt in the carbonates does not have a pristine composition but is altered due to interaction with the carbonates. The low SiO_2 content of this residual melt could be explained by reaction with dolomite to form clinopyroxene. The consumption of dolomite to produce garnet and clinopyroxene in reaction (1) liberates a great amount of CO_2. We suggest that CO_2 is bound in a carbonate melt which produces the polyphase carbonate inclusions. This carbonate melt could contain high amounts of H_2O and potentially also contained alkalis. The carbonate inclusions are often associated with silicate minerals such as phengite, titanite, allanite, biotite and K-feldspar. This might indicate that there is a considerable solubility of silicate minerals in such hydrous carbonate melts. Pal'yanov et al., [48] have shown that silicate phases crystallise from carbonate melts at high pressure and temperatures in agreement with our textural observations. The observed features in the marbles are very similar to results from sandwich experiments at 950–1000 °C, 4.5 GPa reported by Hermann and Green [49,50]. A small layer of dolomite has been embedded in pelites, which underwent partial melting at the experimental conditions. The hydrous granitic melt derived from the pelite layer reacted with the dolomite layer and produced garnet and clinopyroxene. Qualitative mass balance calculations revealed that after reaction there was a liquid present in the dolomite layer consisting mainly of CO_2, with minor amounts of H_2O, K_2O and CaO and very small amounts of SiO_2, MgO and Al_2O_3. The good agreement of these experimental results with the observed textures in the marbles provides further evidence that carbonate melts are produced within the marbles whereas the silicate melt likely derives from the adjacent metapelites.

6.3. Diamond genesis

Detailed infrared spectroscopy of diamond from carbonate rocks revealed the presence of fluid inclusions containing both CO_2 and H_2O [13]. This supports our observation that diamond is closely associated with carbonate and silicate melt inclusions (Fig. 2). Diamonds extracted from a dolomite marble have a high N content (2650 ppm) and $\delta^{15}N$ of 8.5 suggesting that N derived from the adjacent gneisses is involved in diamond formation [51]. This supports our interpretation that hydrous silicate melts sourced from the gneisses interact with the marbles at diamond facies conditions. Some of the diamonds found in the polyphase magnesian carbonate inclusions can be considered as daughter crystals derived from a crystallising carbonate melt. However, the carbonate–diamond ratio varies significantly in different inclusions. In some inclusions diamond occupies more than 90% of the total volume of an inclusion indicating that a significant portion of diamonds grew contemporary with the host garnet and clinopyroxene as a reaction product and not necessarily as precipitates during cooling from a trapped melt. In a reaction of silicate melts with carbonates such as shown in Eq. (1) it is likely that some of the CO_2 liberated by the consumption of carbonate is reduced to form diamond, whereas some diamond might directly precipitate from dissolved C in such melts. This is in agreement with the $\delta^{13}C$ of −10.5 of diamond from the marbles, which show an intermediate composition between carbonate and organic carbon [51]. The presence of melts with different chemical characteristics (Fig. 8) might explain why diamonds with liquid inclusions display a wide range of trace element patterns (e.g. [52]). Diamond is often found in marbles containing K-rich clinopyroxene whereas it is generally absent in marbles with K-poor ($K_2O < 0.1$ wt.%) clinopyroxene [53]. We have shown that K-rich clinopyroxene is likely a product of interaction between hydrous silicate melts with carbonates. Therefore we suggest that such an interaction promotes diamond growth.

Generally, graphite coats around diamonds are interpreted to represent partial retrogression of diamonds [14,33,38,39,53]. We find such graphite-coated diamonds also associated with carbonate inclusions that do not display evidence of retrograde alteration and that form rosettes, which are hard to reconcile with a retrograde alteration of diamond. Additionally, the diamond and graphite aggregates can be significantly larger than the unaltered single diamonds (Fig. 4e), which is not consistent with a retrograde replacement of diamond with graphite. An alternative explanation could be that this represents a co-precipitation of diamond and graphite [54,55].

The involvement of hydrous granitic melt in the formation of metamorphic diamond in the Erzgebirge has been proposed by Hwang et al. [15], Stöckhert et al. [16] and Massonne [12] on the basis of inclusion relationships similar to what is presented here. Additionally to silicate melts, our study provides for the first time evidence, that also carbonate melts were involved in the formation of metamorphic diamonds. This is in excellent agreement with recent experimental studies demonstrating that diamond can form directly from carbonate melts [48,56,57]. In the experiments, carbonate melt dissolves up to 0.3 wt.% of carbon (at $P = 5.7$ GPa and $T = 1470$ °C, [5]), which might precipitate as diamond and/or graphite depending on the conditions

of crystallisation of the melt. Additionally, experiments showed that at relatively low temperatures (1300 °C) diamond and graphite can crystallise contemporary, while at high temperature experiments (>1500 °C) only diamond forms [58,59]. These experiments are in line with our observation suggesting that the presence of graphite is not necessarily a retrograde feature and might represent a co-precipitation with diamond in some of the melt inclusions.

6.4. Consequences for subduction zone processes

Formation of carbonate melts has been generally restricted to mantle melting [1,2,60] and has not been reported from exhumed high-pressure rocks from former subduction zones. There has been indirect evidence from metasomatised mantle wedge xenoliths that silicate–carbonate melts might be generated in subducted crust [61]. Also, it has been suggested from the isotopic signature of carbonatites that carbonate liquids derived from subducted sediments are likely to be involved in the formation of carbonatites [62]. In this study we have shown that hydrous carbonate melts can form when hydrous silicate melts interact with carbonates at high pressure. Interlayered carbonate-pelite rocks are very common in subducted sediments and hence the production of silicate and carbonate melts as observed in the Kokchetav marbles might be a common phenomenon in the sub-arc region of subduction zones. Our data show that such carbonate melts might have slightly higher HREE and significantly higher LREE and Sr contents than silicate melts, but most importantly are able to transfer significant amounts of CO_2 from the subducted slab into the mantle wedge. Such a process has not yet been considered in the modelling of CO_2 recycling subduction zone [63]. Further studies must investigate how such carbonate melts interact with other subducted rocks and how they interact with mantle rocks to clarify the importance of such melts for trace element and volatile transfer in subduction zones.

7. Conclusions

(1) Magnesian calcite inclusions in peak metamorphic garnet and clinopyroxene within UHP marbles display typical textures of melt inclusions. They have a completely different REE pattern compared with matrix magnesian calcite (higher LREE, lower HREE, much higher Ba), which supports an origin as trapped melts. This represents the first direct evidence for carbonate melts in deeply subducted crust.

(2) Primary carbonate melts formed in subducted crust are Ca-rich and Mg-poor in composition and are likely to be hydrous. Such melts are able to transport significant amounts of C from the slab to the mantle wedge and might provoke carbonate and diamond formation in the mantle. Because the carbonate melts contain high contents of Sr and Pb, such melts might add a distinct Pb and Sr isotope signature to the mantle wedge.

(3) Textures and trace element compositions of polyphase silicate inclusions and K-rich clinopyroxene indicate that the investigated marbles interacted with hydrous granitic melts derived from adjacent metapelites during ultra high-pressure metamorphism.

(4) Diamond has been found as inclusion in garnet and clinopyroxene as well as in former silicate and carbonate melt inclusions. This suggests that multiple processes such as the interaction of different melt types and the cooling of carbon saturated melts might produce metamorphic diamonds. Our findings provide strong evidence that the presence of melts promotes diamond growth in deeply subducted crust.

Acknowledgments

We would like to thank the crew from the Electron Microscope Unit (ANU) for help with the SEM and C. Allen and M. Shelley for their assistance at the laser ablation ICP-MS. Comments of D. Rubatto and reviews by H.J. Massone, P. Philippot, J. Blundy and anonymous reviewer helped to improve the paper. Our work on UHPM greatly benefited from encouraging support and the many fruitful discussions with K. Theunissen and Academician N.L. Dobretsov. This work was financially supported by Russian Foundation for Basic Research (04-05-64360-a), Belgian Government BOSTCA, the Schweizerischer Nationalfonds and the Australian Research Council.

Appendix A. Supplementary data

Supplementary data associated with this article can be found, in the online version, at doi:10.1016/j.epsl.2005.10.037.

References

[1] P. Schiano, R. Clocchiatti, N. Shimizu, D. Weis, N. Mattielli, Cogenetic silica-rich and carbonate-rich melts trapped in mantle minerals in Kerguelen ultramafic xenoliths: implications for

metasomatism in the oceanic upper mantle, Earth Planet. Sci. Lett. 123 (1994) 167–178.
[2] M.L. Frezzotti, J.L.R. Touret, E.R. Neumann, Ephemeral carbonate melts in the upper mantle: carbonate–silicate immiscibility in microveins and inclusions within spinel peridotite xenoliths, La Gomera, Canary Islands, Eur. J. Mineral. 14 (2002) 891–904.
[3] L.N. Kogarko, G. Kurat, T. Ntaflos, Carbonate metasomatism of the oceanic mantle beneath Fernando de Noronha Island, Brazil, Contrib. Mineral. Petrol. 140 (2001) 577–587.
[4] M. Akaishi, H. Kanda, S. Yamaoka, Synthesis of diamond from graphite carbonate systems under very high temperature and pressure, J. Cryst. Growth 104 (1990) 578–581.
[5] Y.N. Pal'yanov, A.G. Sokol, Y.M. Borzdov, A.F. Khokhryakov, Fluid-bearing alkaline carbonate melts as the medium for the formation of diamonds in the Earth's mantle: an experimental study, Lithos 62 (2002) 145–159.
[6] D.H. Green, M.E. Wallace, Mantle metasomatism by ephemeral carbonate melts, Nature 336 (1988) 459–462.
[7] G.M. Yaxley, D.H. Green, V. Kamenetsky, Carbonatite metasomatism in the Southeastern Australian lithosphere, J. Petrol. 39 (1998) 1917–1930.
[8] J. Adam, T.H. Green, S.H. Sie, C.G. Ryan, Trace element partitioning between aqueous fluids, silicate melts and minerals, Eur. J. Mineral. 9 (1997) 569–584.
[9] N.V. Sobolev, V.S. Shatsky, Diamond inclusions in garnets from metamorphic rocks: a new environment for diamond formation, Nature 343 (1990) 742–746.
[10] H. Becker, R. Altherr, Evidence from ultra-high-pressure marbles for recycling of sediments into the mantle, Nature 358 (1992) 745–748.
[11] H.L.M. van Roermund, D.A. Carswell, M.R. Drury, T.C. Heijboer, Micro-diamonds in a megacrystic garnet websterite pod from Bardane on the island of Fjortoft, Western Norway: evidence for diamond formation in mantle rocks during deep continental subduction, Geology 30 (2002) 959–962.
[12] H.-J. Massonne, A comparison of the evolution of diamondiferous quartz-rich rocks from the Saxonian Erzgebirge and the Kokchetav massif: are so-called diamondiferous gneisses magmatic rocks?, Earth Planet. Sci. Lett. 216 (2003) 347–364.
[13] K. De Corte, P. Cartigny, V.S. Shatsky, N.V. Sobolev, M. Javoy, Evidence of fluid inclusions in metamorphic microdiamonds from the Kokchetav massif, northern Kazakhstan, Geochim. Cosmochim. Acta 62 (1998) 3765–3773.
[14] L.F. Dobrzhinetskaya, H. Green, K. Bozhilov, T. Mitchell, R. Dickerson, Crystallization environment of Kazakhstan microdiamond: evidence from nanometric inclusions and mineral associations, J. Metamorph. Geol. 21 (2003) 425–437.
[15] S.-L. Hwang, P. Shen, H.-T. Chu, T.-F. Yui, C.-C. Lin, Genesis of microdiamonds from melt and associated multiphase inclusions in garnet of ultrahigh-pressure gneiss from Erzgebirge, Germany, Earth Planet. Sci. Lett. 188 (2001) 9–15.
[16] B. Stöckhert, J. Duyster, C. Trepmann, H.-J. Massonne, Microdiamond daughter crystals precipitated from supercritical C–O–H fluids included in garnet, Erzgebirge, Germany, Geology 29 (2001) 391–394.
[17] O.M. Rozen, Y.M. Zorin, A.A. Zayachkovsky, A find of diamond linked with eclogites of the Precambrian Kokchetav massif, Dokl. Akad. Nauk SSSR 203 (1972) 674–676 (in Russian).
[18] N.L. Dobretsov, N.V. Sobolev, V.S. Shatsky, R.G. Coleman, W.G. Ernst, Geotectonic evolution of diamondiferous paragneisses of the Kokchetav complex, Northern Kazakhstan—the geologic enigma of ultrahigh-pressure crustal rocks within Phanerozoic foldbelt, Isl. Arc 4 (1995) 267–279.
[19] W.R. Taylor, D. Canil, H.J. Milledge, Kinetics of ib to IaA nitrogen aggregation in diamond, Geochim. Cosmochim. Acta 60 (1996) 4725–4733.
[20] J. Hermann, D. Rubatto, A. Korsakov, V.S. Shatsky, Multiple zircon growth during fast exhumation of diamondiferous, deeply subducted continental crust (Kokchetav massif, Kazakhstan), Contrib. Mineral. Petrol. 141 (2001) 66–82.
[21] J. Hermann, Carbon recycled into deep Earth: evidence from dolomitic dissociation in subduction-zone rocks: comment, Geol. Forum (2003) e4–e5.
[22] D. Canil, Experimental study bearing on the absence of carbonate in mantle-derived xenoliths, Geology 18 (1990) 1011–1013.
[23] V.S. Shatsky, N.V. Sobolev, M.A. Vavilov, Diamond-bearing metamorphic rocks of the Kokchetav massif (northern Kazakhstan), Ultrahigh Pressure Metamorphism, R.G. Coleman and X. Wang Edition, Cambridge University Press, Cambridge, 1995, pp. 427–455.
[24] V.S. Shatsky, E. Jagoutz, N.V. Sobolev, O.A. Kozmenko, V.S. Parkhomenko, M. Troesch, Geochemistry and age of ultrahigh pressure metamorphic rocks from the Kokchetav massif (Northern Kazakhstan), Contrib. Mineral. Petrol. 137 (1999) 185–205.
[25] N.V. Sobolev, V.S. Shatsky, M.A. Vavilov, S.V. Goryainov, Zircon of high-pressure metamorphic rocks from folded regions as a unique container of inclusions of diamond, coesite, and coexisting minerals, Dokl. Akad. Nauk SSSR 334 (1994) 488–492.
[26] K. Theunissen, N.L. Dobretsov, A. Korsakov, A. Travin, V.S. Shatsky, L. Smirnova, A. Boven, Two contrasting petrotectonic domains in the Kokchetav megamelange (north Kazakhstan): difference in exhumation mechanisms of ultrahigh-pressure crustal rocks, or a result of subsequent deformation?, Isl. Arc 9 (2000) 428–438.
[27] K. Theunissen, N.L. Dobretsov, V.S. Shatsky, L. Smirnova, A. Korsakov, The diamond-bearing Kokchetav UHP massif in Northern Kazakhstan: exhumation structure, Terra Nova 12 (2000) 181–187.
[28] J.C. Claoue-Long, N.V. Sobolev, V.S. Shatsky, A.V. Sobolev, Zircon response to diamond-pressure metamorphism in the Kokchetav massif, USSR, Geology 19 (1991) 710–713.
[29] I. Katayama, S. Nakashima, Hydroxyl in clinopyroxene from the deep subducted crust: evidences for H_2O transport into the mantle, Am. Mineral. 88 (2001) 229–234.
[30] H. Massago, Metamorphic petrology of the Barchi-Kol metabasites, western Kokchetav ultrahigh-pressure–high-pressure massif, northern Kazakhstan, Isl. Arc 9 (2000) 358–378.
[31] A.V. Korsakov, V.S. Shatsky, N.V. Sobolev, The first finding of coesite in eclogites of the Kokchetav massif, Dokl. Akad. Nauk 360 (1998) 77–81.
[32] A.V. Korsakov, V.S. Shatsky, N.V. Sobolev, A.A. Zayachkovsky, Garnet–biotite–clinozoisite gneisses: a new type of diamondiferous metamorphic rocks of the Kokchetav massif, Eur. J. Mineral. 14 (2002) 915–929.
[33] Y.F. Zhu, Y. Ogasawara, Carbon recycled into the deep Earth: evidenced by dolomite dissociation in subduction-zone rocks, Geology 30 (2002) 947–950.
[34] S.M. Eggins, R.L. Rudnick, W.F. McDonough, The composition of peridotites and their minerals: a laser ablation ICP-MS study, Earth Planet. Sci. Lett. 154 (1998) 53–71.
[35] N.J.G. Pearce, W.T. Perkins, J.A. Westgate, M.P. Gorton, S.E. Jackson, C.R. Neal, S.P. Chenery, A compilation of new and

published major and trace element data for NIST SRM 610 and NIST SRM 612 glass reference materials, Geostand. Newsl. 21 (1997) 115–144.
[36] R. Kretz, Symbols of rock-forming minerals, Am. Mineral. 68 (1983) 277–279.
[37] L.L. Perchuk, O.G. Safonov, V.O. Yapaskurt, J.M.B. Jr., Crystal-melt equilibria involving potassium-bearing clinopyroxene as indicator of mantle-derived ultrahigh-potassic liquids: an analytical review, Lithos 60 (2002) 89–111.
[38] Y. Ogasawara, M. Ohta, K. Fukasawa, I. Katayama, S. Maruyama, Diamond-bearing and diamond-free metacarbonate rocks from Kumdy-Kol in the Kokchetav massif, northern Kazakhstan, Isl. Arc 9 (2000) 400–416.
[39] R.Y. Zhang, J.G. Liou, W.G. Ernst, R.G. Coleman, N.V. Sobolev, V.S. Shatsky, Metamorphic evolution of diamond-bearing and associated rocks from Kokchetav massif, northern Kazakhstan, J. Metamorph. Geol. 15 (1997) 479–496.
[40] Y. Ogasawara, K. Fukasawa, S. Maruyama, Coesite exsolution from supersilicic titanite in UHP marble from the Kokchetav massif, northern Kazakhstan, Am. Mineral. 87 (2002) 454–461.
[41] S.-L. Hwang, P. Shen, H.-T. Chu, T.-F. Yui, J.G. Liou, N.V. Sobolev, R.-Y. Zhang, V.S. Shatsky, A. Zayachkovsky, Kokchetavite: a new potassium-feldspar polymorph from the Kokchetav ultrahigh-pressure terrane, Contrib. Mineral. Petrol. 148 (2004) 380–389.
[42] G.E. Harlow, R. Davies, Status report on stability of K-rich phases at mantle conditions, Lithos 77 (2004) 647–653.
[43] J.A. Dalton, D.C. Presnall, The continuum of primary carbonatitic–kimberlitic melt compositions in equilibrium with lherzolite: data from the system $CaO–MgO–Al_2O_3–SiO_2–CO_2$ at 6 GPa, J. Petrol. 39 (1998) 1953–1964.
[44] W.-J. Lee, P.J. Wyllie, Processes of crustal carbonatite formation by liquid immiscibility and differentiation, elucidated by model systems, J. Petrol. 39 (11-12) (1998) 2005–2013.
[45] R. Dasgupta, M.M. Hirschmann, A.C. Withers, Deep global cycling of carbon constrained by the solidus of anhydrous, carbonated eclogite under upper mantle conditions, Earth Planet. Sci. Lett. 227 (2004) 73–85.
[46] T. Hammouda, High-pressure melting of carbonated eclogite and experimental constraints on carbon recycling and storage in the mantle, Earth Planet. Sci. Lett. 214 (2003) 357–368.
[47] G.M. Yaxley, G.P. Brey, Phase relations of carbonate-bearing eclogite assemblages from 2.5 to 5.5 GPa: implications for petrogenesis of carbonatites, Contrib. Mineral. Petrol. 146 (2004) 606–619.
[48] Y.N. Pal'yanov, V.S. Shatsky, A.G. Sokol, A.A. Tomilenko, N.V. Sobolev, Crystallization of metamorphic diamond: an experimental modeling, Dokl. Earth Sci. 381 (2001) 935–938.
[49] J. Hermann, D.H. Green, Experimental constraints on melt–carbonate interaction at UHP conditions: a clue for metamorphic diamond formation?, Fluid/Slab/Mantle Interactions and Ultrahigh-P Minerals. Abstracts of UHPM Workshop 2001, Waseda University, 2001, pp. 31–34.
[50] J. Hermann, D.H. Green, Interaction of hydrous granitic melts with carbonates: implications for devolatilisation in subduction zones, EMPG IX Ninth International Symposium on Experimental Mineralogy, Petrology and Geochemistry Abstract 7, 2002, p. 44.
[51] P. Cartigny, K. De Corte, V.S. Shatsky, M. Ader, P. De Paepe, N.V. Sobolev, M. Javoy, The origin and formation of metamorphic microdiamonds from the Kokchetav massif, Kazakhstan: a nitrogen and carbon isotopic study, Chem. Geol. 176 (2001) 265–281.
[52] K. De Corte, A. Korsakov, W.R. Taylor, P. Cartigny, M. Ader, P. De Paepe, Diamond growth during ultrahigh-pressure metamorphism of the Kokchetav massif, northern Kazakhstan, Isl. Arc 9 (2000) 284–303.
[53] H.-P. Schertl, N.V. Sobolev, R.D. Neuser, V.S. Shatsky, HP-metamorphic rocks from Dora Maira/Western Alps and Kokchetav/Kazakhstan: new insights using cathodoluminescence petrography, Eur. J. Mineral. 16 (2004) 49–57.
[54] A.V. Korsakov, K. Theunissen, L.V. Smirnova, Intergranular diamonds derived from partial melting of crustal rocks at ultrahigh-pressure metamorphic conditions, Terra Nova 16 (2004) 146–151.
[55] A.V. Korsakov, V.S. Shatsky, Origin of graphite-coated diamonds from the UHP metamorphic rocks, Dokl. Earth Sci. 399 (2004) 1160–1163.
[56] M. Akaishi, H. Kanda, S. Yamaoka, Synthesis of diamond from graphite–carbonate system under very high temperature and pressure, J. Cryst. Growth 104 (1990) 578–581.
[57] A.G. Sokol, A.A. Tomilenko, Y.N. Palyanov, Y.M. Borzdov, G.A. Palyanova, A.F. Khokhryakov, Fluid regime of diamond crystallisation in carbonate–carbon systems, Eur. J. Mineral. 12 (2000) 367–375.
[58] A.G. Sokol, Y.M. Borzdov, Y.N. Pal'yanov, A.F. Khokhryakov, N.V. Sobolev, An experimental demonstration of diamond formation in the dolomite–carbon and dolomite–fluid–carbon systems, Eur. J. Mineral. 13 (2001) 893–900.
[59] A.G. Sokol, Y.N. Pal'yanov, G.A. Pal'yanova, A.F. Khokhryakov, Y.M. Borzdov, Diamond and graphite crystallization from COH fluids under high pressure and high temperature conditions, Diamond Relat. Mater. 10 (2001) 2131–2136.
[60] M. Schrauder, O. Navon, Hydrous and carbonatitic mantle fluids in fibrous diamond from Jwaneng, Botswana, Geochim. Cosmochim. Acta 58 (1994) 761–771.
[61] B.I.A. McInnes, E.M. Cameron, Carbonated, alkaline hybridizing melts from a sub-arc environment: mantle wedge samples from the Tabar–Lihir–Tanga–eni arc, Papua New Guinea, Earth Planet. Sci. Lett. 122 (1994) 125–141.
[62] K. Hoernle, G. Tilton, M.J. Le Bas, S. Duggen, D. Garbe-Schonberg, Geochemistry of oceanic carbonatites compared with continental carbonatites: mantle recycling of oceanic crustal carbonate, Contrib. Mineral. Petrol. 142 (2002) 520–542.
[63] D.M. Kerrick, J.A.D. Conolly, Metamorphic devolitilisation of subducted oceanic metabasalts: implications for seismicity, arc magmatism and volatile recycling, Earth Planet. Sci. Lett. 189 (2001) 19–29.
[64] S.-S. Sun, W.F. McDonough, Chemical and isotopic systematics of oceanic basalts: implications for mantle composition and processes, in: A.D. Saunders, M.J. Norry (Eds.), Magmatism in the Ocean Basin, Geological Society Special Publication, London, Geological Society Special Publication, London, 1989, pp. 313–345.
[65] W.F. McDonough, S.-S. Sun, Composition of the Earth, Chem. Geol. 120 (1995) 223–253.